Published in final edited form as:
Acoust Today. 2012 October 1; 8(4): 15–23. doi:10.1121/1.4788648.

PHOTOACOUSTIC IMAGING FOR MEDICAL DIAGNOSTICS

Carolyn L. Bayer,
Department of Biomedical Engineering, The University of Texas at Austin Austin, Texas 78712

Geoffrey P. Luke, and
Department of Electrical and Computer Engineering, The University of Texas at Austin Austin, Texas 78712

Stanislav Y. Emelianov
Departments of Biomedical and Electrical and Computer Engineering, The University of Texas at Austin Austin, Texas 78712

Introduction

Photoacoustic imaging has the potential to provide real-time, non-invasive diagnosis of numerous prevalent diseases, due to the technology's unique ability to visualize molecular changes deep within living tissue with spatial resolution comparable to ultrasound. Photoacoustic imaging is a hybrid imaging technique that combines the contrast capabilities and spectral sensitivities of optical imaging with the resolution and tissue penetration capabilities of ultrasound. During the photoacoustic imaging process, materials absorb light energy, and convert the light to heat via non-radiative relaxation. When materials heat, they expand in size due to their thermoelastic properties, which generates a pressure wave. These pressure waves can propagate through the surrounding environment to be detected at the surface. This effect is familiar to everyone who has experienced a summer thunderstorm—lightning rapidly heats the air, resulting in the air expanding and generating audible thunder. In general, the heating which induces the expansion of the material (e.g., the thermoacoustic effect) could be caused by many forms of energy transfer, but the term "photoacoustic" specifies the conversion of light into heat, resulting in the generation of characteristic sound waves.

The photoacoustic effect was first discovered by Alexander Graham Bell in 1880.[1] His experiments deduced that an intermittent bright light could heat optically absorbing materials, causing expansion of the material in a way that generated audible vibrational waves. Bell demonstrated that darker fibers produced louder sounds than lighter fibers, a principle which is consistent with the general photoacoustic relationship in use today—the amplitude of the generated photoacoustic signal is proportional to the amount of absorbed light. Bell also showed, by separating white light with a prism, certain color combinations of light and fibers could generate a louder sound. Today, multiwavelength photoacoustic imaging uses this same principle, changing the wavelength of the light and correlating the amplitude of the photoacoustic response to the absorption spectra of the materials being imaged.

A modern application of the photoacoustic effect is the generation of medical images of biological chromophores typically present in tissue, which can absorb light energy resulting in the generation of photoacoustic transients. The photoacoustic pressure waves can be received by ultrasound transducers at the external surface of the tissue, making photoacoustic imaging a non-invasive, non-ionizing medical imaging method capable of resolution similar to ultrasound, at significant tissue depth. Photoacoustic medical imaging was first proposed in the mid-1990s,[2,3] and initial reports of using the photoacoustic effect

to image live animals were published nine years later.[4] Today, many *in vivo* demonstrations of photoacoustic imaging of biomedical applications relevant to medical diagnostics exist, including cancer,[5,6] brain vasculature and function,[7–9] cardiovascular,[10] and tissue engineering scaffolds,[11,12] prompting translational advances in clinical photoacoustic imaging.[13]

While existing medical imaging methods, including ultrasound, are capable of producing remarkable images of what lies beneath our skin, most of these imaging methods provide contrast between anatomical features within tissue—for example, the difference in acoustic impedance between soft tissue and a tumor provide contrast within an ultrasound image. Though the anatomy is critical to understanding the image, in many diseases the anatomy alone cannot be used to indicate a particular diagnosis conclusively. Instead, the physiological and biochemical properties of the system influence the disease progression, and therefore the prognosis of the patient. Functional imaging capabilities are required to provide physiological information, while biochemical information can be provided by molecular imaging. In comparison to ultrasound, photoacoustic imaging provides improved capabilities for functional and molecular imaging. For example, the blood oxygen saturation, an important functional property relevant to many disease processes, can be assessed using photoacoustics.[7] Photoacoustic imaging can also provide molecular information through the use of a probe or tracer, which can be used to generate the needed contrast to produce an image.[14] Because of the potential to perform real-time, non-invasive *in vivo* functional and molecular imaging, photoacoustic imaging is increasingly being applied as both a clinical and preclinical method aimed at improving medical diagnostics.

Background

In a contemporary photoacoustic imaging system, a nanosecond pulsed laser is used to generate transient pressure waves, which are received by an ultrasound transducer and processed to form images of biological tissue (Fig. 1). In a typical set-up, the pulse of light emitted by the laser is accompanied by a trigger signal sent to the imaging system hardware, coordinating the acquisition of the photoacoustic signal. After the laser pulse is emitted, the photoacoustic signals generated by the optical absorbers within the field of view are collected by the transducer (Fig 2). As with ultrasound, the time at which the photoacoustic signal is received is related to the depth of the absorbing object within the sample by the speed of sound in tissue.

Multimodal systems, combining ultrasound and photoacoustic imaging, apply a time delay (τ_{PA}) after the laser trigger signal, as shown in Fig. 2, after which the ultrasound signal is transmitted and received to be processed using customary techniques. Due to the similarities in system hardware and processing design between photoacoustic and ultrasound imaging, an existing ultrasound system can be modified to acquire photoacoustic signals with nominal effort by adding a pulsed light source, making minor hard-ware modifications to appropriately time the transmitted and received signals, and by modifying the software user interface and signal processing methods.

Several companies are marketing integrated photoacoustic systems for small animal imaging, shown in Fig. 3, and it is likely that more will soon enter the market. These systems fall into two categories—designed to use either a translatable linear ultrasound scanner with delay-and-sum beamforming, or a fixed array of transducers with computed tomography image reconstruction. Linear photoacoustic scanning systems produce a two-dimensional (2D) view of a single projection, and are then scanned in a third dimension – a volumetric imaging method analogous to commonly used non-invasive clinical ultrasound systems, where a transducer array is manually scanned along the tissue surface.

Tomographic systems use an array of transducers, often positioned in a ring around the object being imaged, and then use reconstruction algorithms to reproduce the imaged slice. Visual Sonics Inc. markets the Vevo LAZR (Fig. 3a), which uses their high resolution small animal ultrasound imaging platform (Vevo 2100) in combination with a tunable nanosecond pulsed laser. When whole body imaging is a priority, the multispectral optoacoustic tomography (MSOT) system (Fig. 3b), produced by iThera Medical, guides the laser beam to illuminate a ring of light around the animal being imaged, and then moves in the third dimension to acquire volumetric images.[15] The Nexus 128 (Fig. 3c), produced by Endra, provides an alternative tomographic photoacoustic system. All of these systems consist of a tunable laser source providing near infrared (NIR) light approximately between 680 to 970 nm. The choice of a scanning or tomographic system depends greatly upon the application. The user must consider the achievable resolution, which is dependent upon the center frequency and bandwidth of the transducer, the beamforming or reconstruction algorithms implemented, and also the achievable sensitivity, which is influenced by the light fluence and distribution delivered within the tissue. An ultrasound scanning system will generally be most flexible, accommodating a variety of animal types, and potentially providing multiple transducer arrays optimized for different scanning depths. A photoacoustic imaging system based upon an ultrasound scanner platform provides additional functional imaging techniques (such as ultrasound Doppler mode) to provide anatomical and functional information. In contrast, tomographic systems are capable of acquiring volumetric data in a shorter period of time, and have less noise in the form of photoacoustic speckle due to the spatial distribution of the transducer ring. However, clinical applications of a photoacoustic tomography system will be limited, with a notable exception being the photoacoustic tomographic imaging of breast tissue.[16]

While optical absorbers naturally found within the body, such as hemoglobin, lipids, and melanin, can be used to generate photoacoustic images, the use of nano-sized imaging contrast agents allows photoacoustic imaging to become a truly “molecular” *in vivo* imaging method.[17,18] Photoacoustic contrast can be enhanced by the use of molecular dyes or chemically synthesized nanoparticles. Inorganic nanoparticles are of particular interest, due to their flexibility with respect to shape, size, and surface chemistry. These characteristics can be optimized for enhanced delivery of the nanoparticles to the tissue of interest, such as cancerous tumors.[19] If the nanoparticle surface is modified by the addition of a targeting moiety, these contrast agents become molecular imaging agents, since the targeted nanoparticles should be preferentially retained within the tissue region expressing the target. In addition, metallic nanoparticles of gold or silver, several examples of which are shown in Fig. 4, have surface plasmon resonance, meaning that the valence electrons of the atoms collectively oscillate at a characteristic frequency. When the incident light is at the same frequency as the surface plasmon resonance, that light is very efficiently absorbed and converted into heat, making metallic nanoparticles excellent contrast agents for photoacoustic imaging. Nanoparticles which are molecularly targeted can be customized for delivery to particular tissues based on size, shape, and surface properties, while the high optical absorption of metallic nanoparticles generates a strong photoacoustic signal and provides high contrast with the surrounding tissue. By using metallic nanoparticles, we can also tune their optical absorption properties to take advantage of the “tissue optical window”. Within this wavelength region, between approximately 600 nm to 1300 nm, the native tissue optical absorption is relatively low, and therefore light can penetrate deeper into tissue, allowing for acquisition of photoacoustic images at significantly greater tissue depths. By imaging at wavelengths which are not highly absorbed in tissues, the photoacoustic effect can be used to generate high resolution molecular images i*n vivo* at significant tissue depth. Questions remain regarding the safety of metallic nanoparticles for use in the human body.[20,21] Indeed, there is much that is still unknown about both their short-term and long-term toxicity, but many groups are studying these effects,[21] and three

clinical studies of gold nanoparticle-based methodologies for treatment of cancer are underway or have been completed.[22] Additionally, photoacoustic imaging could play a role in improving the understanding of the biodistribution and clearance mechanisms affecting the toxicity of nanoparticles.

Diagnostic photoacoustic imaging

In our studies, anatomical, functional, and molecular information was acquired using a combination of ultrasound and multiwavelength photoacoustic imaging of *in vivo* mice bearing cancerous tumors. All methods follow protocols approved by the Institutional Animal Care and Use Committee at the University of Texas at Austin. First, we developed a small animal model of breast cancer which consisted of two tumors established from human breast cancer cell lines with differential cell biomarker expression. For this small animal model, we initiated tumors within the mammary fat pad using injections of BT-474 cancer cells, which over-express the cellular receptor HER2, and MDA-MB-231 cancer cells, which over-express $\alpha_v\beta_3$ integrin, present on the cell surface of epithelial cells of neovasculature. Gold nanorods were chosen as the molecular contrast agent since, in addition to being highly optically absorbing due to surface plasmon resonance effects, their optical absorption spectra can be tuned by changing their aspect ratio.[23] By tuning nanorods to have different peak optical absorption wavelengths, it is possible to distinguish between multiple nanorod contrast agents through multiwavelength photoacoustic imaging.[24] We coated the nanorods with amorphous silica, which improves the gold nanorod thermal stability[25] and the photoacoustic signal generation efficiency.[26] Silica-coated nanorods with two different aspect ratios were chemically modified to attach targeting antibodies, allowing the nanoparticle to be preferentially uptaken by tumor cells over-expressing the targeted cellular receptor.[24] The contrast agents were injected into the bloodstream of a mouse growing the tumors. The injected contrast agents distributed through the circulatory system, and infiltrated through the tissues of the mouse, including the cancerous tumors.

The tumor region of the mouse was imaged using a Vevo 2100 high frequency small animal ultrasound scanner (VisualSonics Inc.), integrated with a SpectraPhysics QuantaRay Pro Nd:YAG nanosecond pulsed laser with a GWU PremiScan optical parametric oscillator (OPO) to tune the light wavelength. A fiber optic bundle was used to deliver the laser light on either side of a linear transducer array. The system was used to deliver between 10–20 mJ/cm^2 of light over a range of wavelengths from 680–930 nm. A 21-MHz ultrasound transducer (MS250, VisualSonics Inc.) collected the photoacoustic signals at each wavelength, followed by the transmission of ultrasound and the receiving of the reflected ultrasound by the same transducer, resulting in co-registered ultrasonic and photoacoustic images. A linear stepper motor was used to translate the transducer and fiber bundle construct, in steps of 150 μm, to acquire photoacoustic and ultrasound images in the third dimension, averaging four photoacoustic signals at each step. Three-dimensional (3D) ultrasound and photoacoustic images were captured in a volume surrounding the two tumors within the mammary fat pad of the mouse.

The amplitude of the photoacoustic signal received is dependent upon the wavelength of the laser light used to illuminate the sample. This dependence can be unmixed into the individual absorption spectra of the absorbers within the tissue—oxyhemoglobin, deoxyhemoglobin, nanoparticle 1 and nanoparticle 2. We used a linear least squared error spectral unmixing method where each voxel was assumed to contain a combination of the four optical absorbers.[27] In this method, the initial photoacoustic signal, located at a position within the image, depends on the concentration of the absorbers in the region, the laser fluence, and the Grüneisen parameter.[28] The optical absorption spectra of hemoglobin were obtained from the literature[29] and the nanoparticle spectra were measured using UV-Vis

spectroscopy (Synergy HT microplate reader, Biotek Instruments, Inc.). If the spectral unmixing problem is over-constrained, which is achieved by acquiring photoacoustic data at more wavelengths than the number of absorbers present in the tissue, then a minimum mean squared error estimate can be obtained for the absorber concentrations. The estimated concentrations of deoxyhemoglobin, oxyhemoglobin, nanoparticle 1, and nanoparticle 2 are displayed using blue, red, green, and violet colormaps, respectively. For spectral unmixing, the data was averaged into voxels of size 500 μm 200 μm 300 μm. The images of the optical absorbers were overlaid on co-registered ultrasound grayscale images to visualize the anatomy in the region.

High resolution 3D anatomical images of the tumor region were generated by processing the ultrasound signals received by the integrated ultrasound and photoacoustic imaging system (Fig. 5). In Fig. 5a, a 3D image of a single wavelength photoacoustic image, overlaid on the ultrasound image, clearly shows the anatomy within the imaged region of the mouse, including the vasculature (in color, provided by the photoacoustic image), and the layer of skin and the femur within the leg (in greyscale, provided by the ultrasound image). In our mouse model we can identify the tumor regions by locating two hypoechoic regions under the skin, as shown in the 2D ultrasound slice in Figure 5b. From the photoacoustic signal (Fig. 5c and 5d), it is clear that there are light absorbers within the skin, light absorption from vasculature surrounding the tumors, and from the tumors themselves. While both ultrasound and photoacoustic images indicate the presence of tumors, the anatomical images alone do not provide sufficient information to diagnose malignancy, since the accuracy of ultrasound in the distinction of benign and malignant tumors is insufficient.[30] While the *in vivo* ultrasound and single wavelength photoacoustic images in Fig. 5 provide high resolution anatomical information, the cellular composition of the tumor is unknown, and thus we are unable, at this stage of imaging, to identify functional characteristics or the cellular molecular expression, which might aid in the identification of a benign versus cancerous tumor.

Functional photoacoustic images, for example of the blood oxygen saturation of the tumor, could provide additional criteria to assess tumor function. We acquired functional information by detecting photoacoustic signals at multiple laser wavelengths and spectrally unmixing the signals as described above. For functional imaging of the animal model described above, we acquired photoacoustic signals generated by laser light between 680–850 nm. As shown in Figure 6, we can observe the oxygen saturation of the blood within the “normal” tissue and within the tumor regions. The estimated concentrations of deoxyhemoglobin and oxyhemoglobin are shown using a color scale ranging from blue (0% oxygen saturation) to red (100% oxygen saturation). The 3D image shown in Figure 6a indicates distinction of venuous flow from arterial flow within vasculature of the imaged tissue. While the study of vasculature has relevance to some niches of medical diagnostics, more significantly, we can use the functional information provided by the multiwavelength photoacoustic imaging to study the tumor blood oxygen saturation. Hypoxic malignant tumors have a worse prognosis, making the blood oxygen saturation useful for the assessment of therapy and therapy response.[31] As shown in Fig. 6b, there is a hypoxic region within the core of the imaged tumor. This lower oxygen saturation is likely due to the high metabolic activity of the cells located within that region, leading to insufficient oxygen delivery within the tumor. Functional photoacoustic imaging of the blood oxygen saturation could be used to study the response of the tumor to therapeutic treatment, non-invasively, in real-time, and over long time periods of tumor growth.

Finally, we can further process the photoacoustic images to view the signal which correlates to the optical absorption spectra of the injected contrast agents. In the studies shown here, we have used silica-coated gold nanorods, but it important to note that a large variety of

contrast agents can be successfully used for molecular photoacoustic imaging;[32] *in vivo* photoacoustic imaging with enhanced contrast has been demonstrated with the FDA-approved dye methylene blue,[33] with gold nanospheres,[27] or with silver nanoplates.[34] As shown in Fig. 7, within our mouse model, regions of nanoparticle accumulation correspond to the tumor regions identified with the ultrasound imaging and the functional photoacoustic imaging of the blood oxygen saturation. Over time, there is an increase in the signal attributed to the nanoparticle contrast agents within the tumor region (Fig. 7b, c). The accumulation of nanoparticles could be due to two effects. It is known that tumors have "leaky" vasculature, enabling the increased delivery of nano-sized particles through the enhanced permeability and retention effect. Additionally, the injected nanoparticles were bioconjugated to antibodies specific for cell receptors over-expressed on cell types used to initiate the tumors, thus it is likely that the active targeting improves the retention of the specific nanoparticles within the tumor region. This example demonstrates how the use of nanoparticles can provide molecular information about the cellular expression of the tumor. In this way, photoacoustics combines the benefits of high-contrast optical resolution of targetable light-interacting probes, with the imaging depth capabilities of ultrasound.

Conclusions

The strength of photoacoustic imaging is in its ability to image functional and molecular changes, at significant tissue depth, in living animals. Researchers have just begun to exploit photoacoustic imaging techniques to enable new discoveries of the functional and molecular characteristics of cancer, cardiovascular disease, and neurological diseases. We envision photoacoustic imaging becoming a critical tool in medical diagnostics and image-guided therapeutics in the future. While most photoacoustic functional imaging applications thus far have used contrast sources which are naturally present, it is also possible to introduce biochemically triggered contrast agents for functional imaging. For example, many dyes exist which change their optical absorption spectra based on pH, or in the presence of an enzyme. By adding an activatable contrast agent, we can use the change in the multiwavelength photoacoustic signal intensity to provide quantitative information about the biochemical environment within tissues, and monitor changes in this environment.

While this article focuses on imaging, it is also of note that a natural synergy exists between photoacoustic imaging and therapy. For example, thermal therapy can be achieved by using a continuous light source to heat the optical absorbers used for photoacoustic contrast, to a temperature which can lead to the destruction of the cells and surrounding tissue.[35] Additionally, multimodal photoacoustic contrast agents can be designed to provide laser-activated delivery of therapeutic molecules, such as by using a temperature-responsive polymer coating,[36] or by using the heat to release covalently-linked therapeutics.[37]

Photoacoustic imaging is not without limitations. Like ultrasound, the resolution will be physically limited by the inverse relationship between the imaging depth and the frequency of the ultrasound—as the frequency increases, resolution also increases, however the signal attenuation is greater at higher frequencies, leading to limitations in imaging depth. Sensitivity is impacted by the scattering of light within tissue, however new techniques to maximize the signal to noise, including improved contrast agents, and varying the laser light characteristics, can help to minimize background signal. Other limitations include the time required to scan—achieving high lateral resolution is dependent upon a narrow beam, which means that the receiving transducer (in scanning systems) or object being imaged (in tomographic systems) must be scanned in a third dimension to widen the field of view. This time limitation does limit the temporal resolution of the functional and molecular information which can be obtained to the timescale of minutes. Currently, only preclinical photoacoustic imaging systems are available commercially, but the additional functional and

molecular information available through this imaging modality will mean its increasing use in preclinical studies, providing the needed research background necessary for clinical adaptations.**AT**

Acknowledgments

The authors acknowledge support from the National Institutes of Health (NIH) under grants F32CA159913 (C.L. Bayer), and F31CA168168 (G.P. Luke). We thank Juili Kevlar for providing the silica-coated gold nanorod TEM images, and Dr. Kimberly Homan for providing the silver plate TEM images. We also thank Shailja Tewari of VisualSonics, Christian Wiest of iThera Medical, and Richard Moss of Endra Life Sciences for providing the pictures compiled in Fig. 3.

References

1. Bell AG. On the production and reproduction of sound by light. Am J Sci. 1880; 20:305–324.
2. Kruger RA. Photoacoustic ultrasound. Med Phys. 1994; 21:127–131. [PubMed: 8164577]
3. Oraevsky AA, Jacques SL, Esenaliev RO, Tittel FK. Time-resolved optoacoustic imaging in layered biological tissues. OSA Proc Advances in Optical Imaging and Photon Migration. 1994; 21:161–165.
4. Wang X, Pang Y, Ku G, Xie X, Stoica G, Wang LV. Noninvasive laser-induced photoacoustic tomography for structural and functional in vivo imaging of the brain. Nature Biotechnol. 2003; 21:803–806. [PubMed: 12808463]
5. Mallidi S, Luke GP, Emelianov S. Photoacoustic imaging in cancer detection, diagnosis, and treatment guidance. Trends in Biotechnol. 2011; 29:213–221.
6. Laufer J, Johnson P, Zhang E, Treeby B, Cox B, Pedley B, Beard P. *In vivo* preclinical photoacoustic imaging of tumor vasculature development and therapy. J Biomed Optics. 2012; 17:056016–1.
7. Stein EW, Maslov K, Wang LV. Noninvasive, in vivo imaging of blood-oxygenation dynamics within the mouse brain using photoacoustic microscopy. J Biomed Optics. 2009; 14:020502–020502.
8. Laufer J, Zhang E, Raivich G, Beard P. Three-dimensional noninvasive imaging of the vasculature in the mouse brain using a high resolution photoacoustic scanner. Appl Optics. 2009; 48:D299–306.
9. Tsytsarev V, Maslov KI, Yao J, Parameswar AR, Demchenko AV, Wang LV. *In vivo* imaging of epileptic activity using 2-nbdg, a fluorescent deoxyglucose analog. J Neurosci Methods. 2012; 203:136–140. [PubMed: 21939688]
10. Taruttis A, Herzog E, Razansky D, Ntziachristos V. Real-time imaging of cardiovascular dynamics and circulating gold nanorods with multispectral optoacoustic tomography. Optics Express. 2010; 18:19592–19602. [PubMed: 20940855]
11. Cai X, Paratala BS, Hu S, Sitharaman B, Wang LV. Multiscale photoacoustic microscopy of single-walled carbon nanotube-incorporated tissue engineering scaffolds. Tissue Engineering Part C Methods. 2012; 18:310–317. [PubMed: 22082018]
12. Nam SY, Ricles LM, Suggs LJ, Emelianov SY. *In vivo* ultrasound and photoacoustic monitoring of mesenchymal stem cells labeled with gold nanotracers. PLoS ONE. 2012; 7:e37267. [PubMed: 22615959]
13. Piras D, Xia W, Steenbergen W, van Leeuwen T, Manohar SG. Imaging breast lesions using the twente photoacoustic mammoscope: Ongoing clinical experience. Proc SPIE. 2012; 8223:82231–82230C.
14. Luke GP, Yeager D, Emelianov SY. Biomedical applications of photoacoustic imaging with exogenous contrast agents. Ann Biomed Eng. 2012; 40:422–437. [PubMed: 22048668]
15. Razansky D, Buehler A, Ntziachristos V. Volumetric real-time multispectral optoacoustic tomography of biomarkers. Nature Protocols. 2011; 6:1121–1129.
16. Kruger RA, Lam RB, Reinecke DR, Del Rio SP, Doyle RP. Photoacoustic angiography of the breast. Med Phys. 2010; 37:6096–6100. [PubMed: 21158321]

17. Agarwal A, Huang SW, O'Donnell M, Day KC, Day M, Kotov N, Ashkenazi S. Targeted gold nanorod contrast agent for prostate cancer detection by photoacoustic imaging. J Appl Phys. 2007; 102
18. Li PC, Wang CRC, Shieh DB, Wei CW, Liao CK, Poe C, Jhan S, Ding AA, Wu YN. *In vivo* photoacoustic molecular imaging with simultaneous multiple selective targeting using antibody-conjugated gold nanorods. Optics Express. 2008; 16:18605–18615. [PubMed: 19581946]
19. Jain RK, Stylianopoulos T. Delivering nanomedicine to solid tumors. Nature Reviews Clinical Oncol. 2010; 7:653–664.
20. Goel R, Shah N, Visaria R, Paciotti GF, Bischof JC. Biodistribution of tnf-alpha-coated gold nanoparticles in an *in vivo* model system. Nanomedicine. 2009; 4:401–410. [PubMed: 19505243]
21. Khlebtsov N, Dykman L. Biodistribution and toxicity of engineered gold nanoparticles: A review of *in vitro* and *in vivo* studies. Chem Soc Rev. 2011; 40:1647–1671. [PubMed: 21082078]
22. Clinicaltrials.gov [Internet]. Bethesda: U.S. National Institutes of Health; 2000. [cited 2012 Sept 1]. Available from: http://www.clinicaltrials.gov/
23. Jain PK, Lee KS, El-Sayed IH, El-Sayed MA. Calculated absorption and scattering properties of gold nanoparticles of different size, shape, and composition: Applications in biological imaging and biomedicine. J Phys Chem B. 2006; 110:7238–7248. [PubMed: 16599493]
24. Bayer CL, Chen YS, Kim S, Mallidi S, Sokolov K, Emelianov S. Multiplex photoacoustic molecular imaging using targeted silica-coated gold nanorods. Biomed Optics Express. 2011; 2:1828–1835.
25. Chen YS, Frey W, Kim S, Homan K, Kruizinga P, Sokolov K, Emelianov S. Enhanced thermal stability of silica-coated gold nanorods for photoacoustic imaging and image-guided therapy. Optics Express. 2010; 18:8867–8878. [PubMed: 20588732]
26. Chen YS, Frey W, Kim S, Kruizinga P, Homan K, Emelianov S. Silica-coated gold nanorods as photoacoustic signal nanoamplifiers. Nano Lett. 2011; 11:348–354. [PubMed: 21244082]
27. Kim S, Chen YS, Luke GP, Emelianov SY. "*In vivo* three-dimensional spectroscopic photoacoustic imaging for monitoring nanoparticle delivery. Biomed Optics Express. 2011; 2:2540–2550.
28. Kim S, Chen YS, Luke GP, Emelianov SY. *In vivo* three-dimensional spectroscopic photoacoustic imaging for monitoring nanoparticle delivery. Biomed Optics Express. 2011; 2:2540–2550.
29. Prahl, S. Optical absorption of hemoglobin. Oregon Medical Laser Center; 1999.
30. Sehgal C, Weinstein S, Arger P, Conant E. A review of breast ultrasound. J Mammary Gland Biology and Neoplasia. 2006; 11:113–123.
31. Harris AL. Hypoxia--a key regulatory factor in tumour growth. Nature Reviews Cancer. 2002; 2:38–47.
32. Luke GP, Yeager D, Emelianov SY. Biomedical applications of photoacoustic imaging with exogenous contrast agents. Ann Biomed Eng. 2012; 40:422–437. [PubMed: 22048668]
33. Song KH, Stein EW, Margenthaler JA, Wang LV. Noninvasive photoacoustic identification of sentinel lymph nodes containing methylene blue *in vivo* in a rat model. J Biomed Optics. 2008; 13:054033.
34. Homan KA, Souza M, Truby R, Luke GP, Green C, Vreeland E, Emelianov S. Silver nanoplate contrast agents for *in vivo* molecular photoacoustic imaging. ACS Nano. 2012; 6:641–650. [PubMed: 22188516]
35. Kim JW, Galanzha EI, Shashkov EV, Moon HM, Zharov VP. Golden carbon nanotubes as multimodal photoacoustic and photothermal high-contrast molecular agents. Nature Nanotechnology. 2009; 4:688–694.
36. Owens DE, Eby JK, Jian Y, Peppas NA. Temperature-responsive polymer–gold nanocomposites as intelligent therapeutic systems. J Biomed Mat Res Part A. 2007; 83A:692–695.
37. Zandberg WF, Bakhtiari ABS, Erno Z, Hsiao D, Gates BD, Claydon T, Branda NR. Photothermal release of small molecules from gold nanoparticles in live cells. Nanomedicine. 2012; 8:908–915. [PubMed: 22100758]

Biographies

Carolyn L. Bayer is a Ruth L. Kirschstein National Research Service Award (NRSA) Postdoctoral Fellow at the University of Texas at Austin. She completed a B.S. in Electrical Engineering at Case Western Reserve University, and a Ph.D in Biomedical Engineering at the University of Texas at Austin. Her postdoctoral research uses multiwavelength photoacoustic imaging, in combination with biomolecularly-targeted nanoparticle contrast agents, to monitor the development of distinctive molecular signatures involved in tumor growth and response to treatment *in vivo*.

Geoffrey Luke is a Ruth L. Kirschstein National Research Service Award (NRSA) Predoctoral Fellow in the Department of Electrical Engineering at The University of Texas at Austin. He received a B.S. in Computer Engineering and Mathematics and a M.S. in Electrical Engineering from the University of Wyoming, where he developed a sensor based on the visual system of the common housefly. His current research is focused on early cancer detection and characterization using molecular photoacoustic imaging.

Stanislav Emelianov received B.S. and M.S. degrees in physics and acoustics in 1986 and 1989, respectively, and a Ph.D. degree in physics in 1993 from Moscow State University, Russia. In 2002, Dr. Emelianov moved to The University of Texas at Austin and formed the Ultrasound Imaging and Therapeutics Research Laboratory. Dr. Emelianov's research interests are in the areas of medical imaging for therapeutics and diagnostic applications, ultrasound microscopy, elasticity imaging, photoacoustical imaging, cellular/molecular imaging, and functional imaging. Dr. Emelianov has published over 100 archival publications and over 12 book chapters. Throughout his career he has mentored and served on dissertation committees of more than 43 graduate students. Finally, Dr. Emelianov is an American Institute for Medical and Biological Engineering (AIMBE) fellow and is currently

Vice President of the Institute of Electrical and Electronics Engineers (IEEE) Ultrasonics, Ferroelectrics and Frequency Control Society.

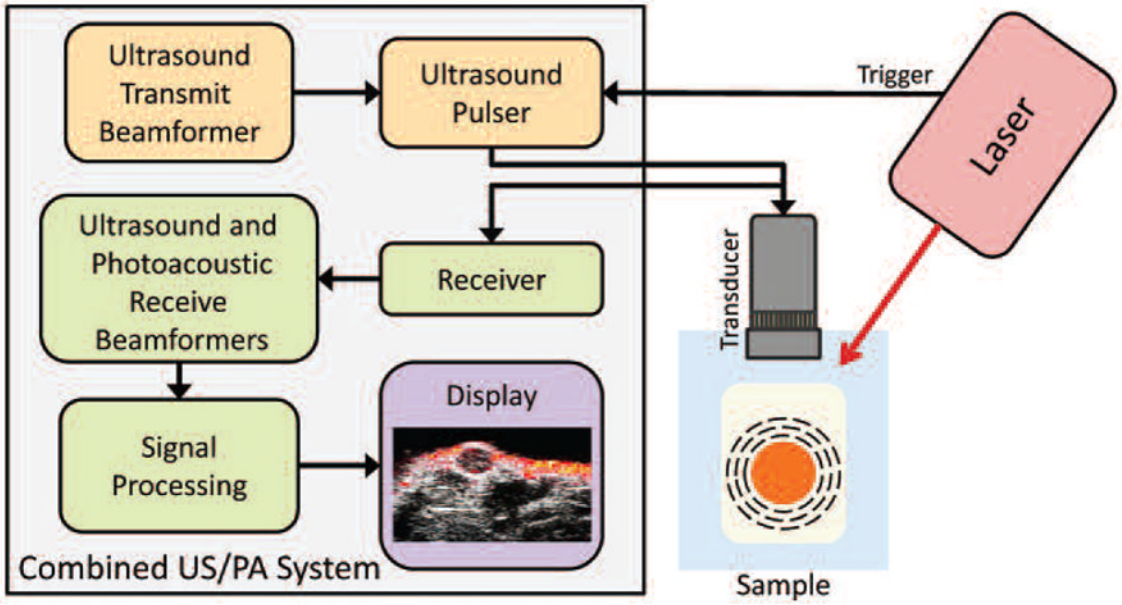

Fig. 1.

Instrumentation and major processing components comprising a combined ultrasound and photoacoustic imaging system. Photoacoustic signal, generated by the optical absorption of laser energy by the sample, is received by an ultrasound transducer, beamformed and processed to form an photoacoustic image. Ultrasound, appropriately beamformed, is emitted by the transducer, and reflected ultrasound is received, beamformed and processed to form the ultrasound image.

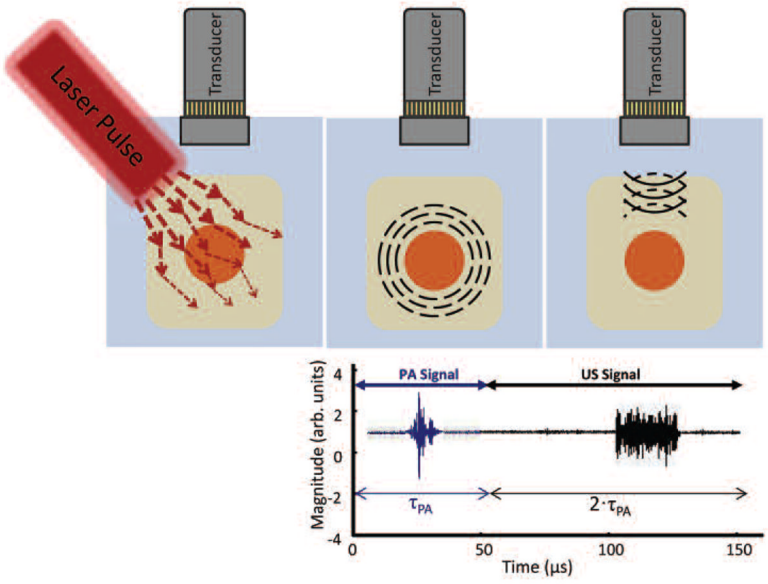

Fig. 2.

Photoacoustic and ultrasound signal generation. (a) The laser pulse is scattered and absorbed by the sample. (b) Absorption which leads to heating generates a transient pressure wave which is received by the transducer. (c) After a delay, τ_{PA}, ultrasound is transmitted and received over the time period $2\cdot\tau_{PA}$.

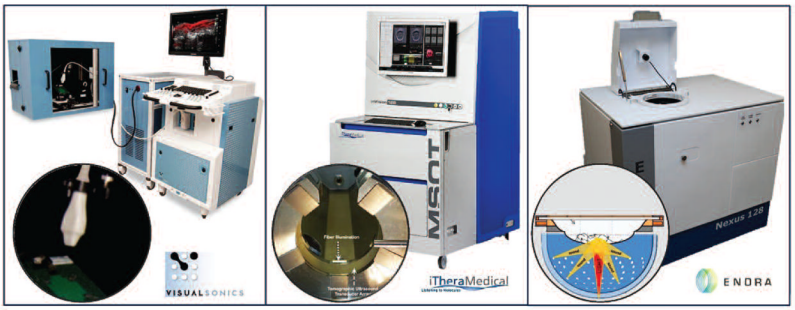

Fig. 3.
Commercially available preclinical photoacoustic imaging systems.

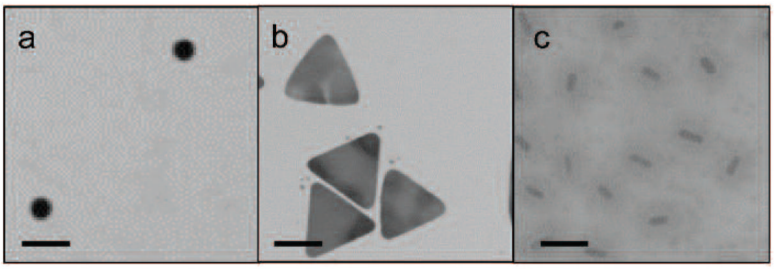

Fig. 4.

Transmission electron microscopy images of plasmonic metallic nanoparticles which have been used for in vivo photoacoustic imaging. (a) Gold nanospheres; (b) Silver nanoplates; (c) Gold nanorods coated with silica. Scale bars = 100 nm.

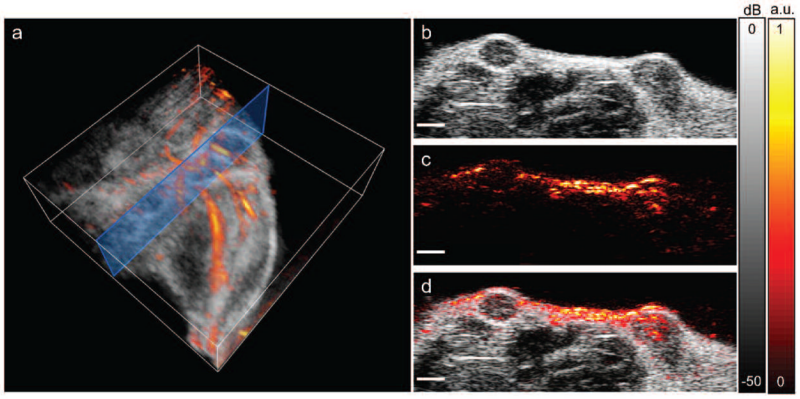

Fig. 5.

In vivo anatomical photoacoustic and ultrasound images. (a) 3D overlay of photoacoustic and ultrasound images of the upper leg/abdominal region. Blue box shows the 2D imaging plane of (b–d). (b) Ultrasound image showing two hypoechoic tumors. (c) Photoacoustic image, acquired using a laser wavelength of 850 nm. (d) Overlay of photoacoustic and ultrasound images. Scale bars = 2 mm.

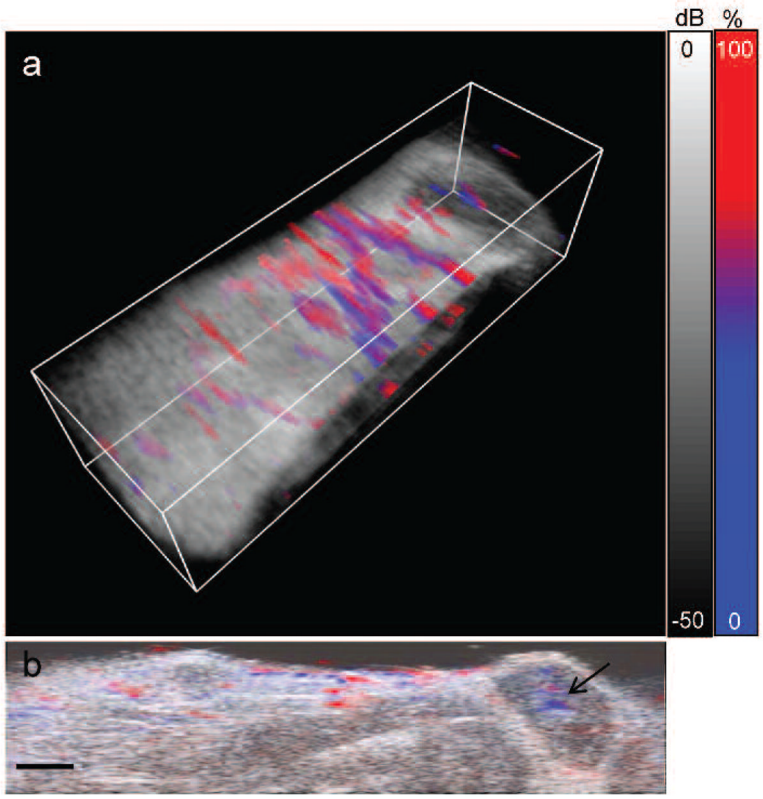

Fig. 6.

In vivo functional imaging of blood oxygen saturation. (a) 3D overlay of percent blood oxygen saturation, determined from spectral unmixing of the multiwavlength photoacoustic signal, and the ultrasound image. Volume is 23 mm (wide) × 6 mm (tall) × 7 mm (scanned direction). (b) 2D slice of the percent blood oxygen saturation and ultrasound signal. Black arrow indicates a hypoxic region within a tumor. Scale bars = 2mm.

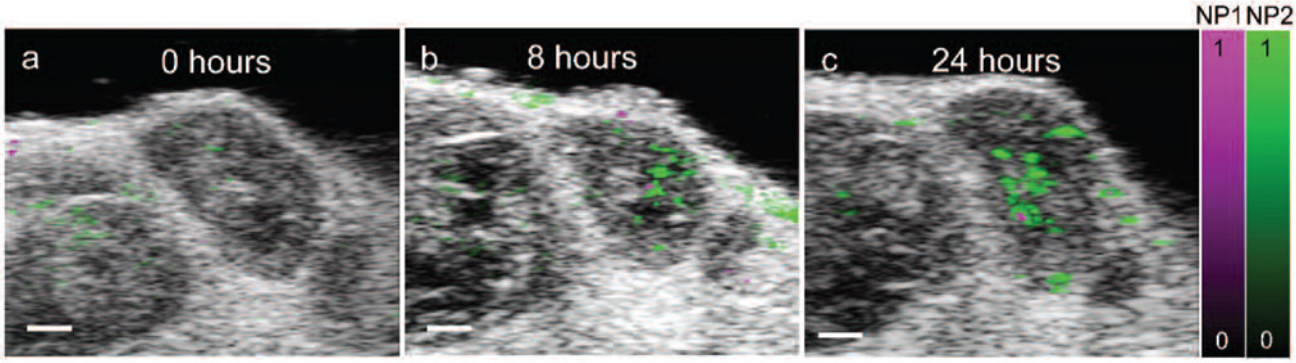

Fig. 7.

In vivo molecular imaging of contrast agent accumulation within a targeted tumor. The multiwavelength photoacoustic signal was unmixed into two components corresponding to two different contrast agents, nanoparticle 1 (NP1) and nanoparticle 2 (NP2). (a) 2D overlay of ultrasound image, distribution of NP1 and NP2 before the injection of the contrast agent, showing minimal background photoacoustic signal. Accumulation of NP1 and NP2 within the tumor is shown (b) 8 hours and (c) 24 hours after intravenous injection. Scale bars = 1 mm.